JCS Journal of Comprehensive Science
JOURNAL OF COMPREHENSIVE SCIENCE
Published by Green Publisher

Journal of Comprehensive Science
p-ISSN: 2962-4738 e-ISSN: 2962-4584
Vol. 3. No. 5, Mei 2024

# Sulfidation of Iron - Based Nanomaterial as Catalyst for Water Splitting Using Hydrothermal

Ni Luh Ayu Ardi Lestari[1], I Gede Arjana[2], Ida Bagus Putu Mardana[3]
Physics Education Department, Faculty Mathematics and Natural Science Ganesha University of Education, Indonesia
Email: ayu.ardi@undiksha.ac.id[1], igede.arjana@undiksha.ac.id[2], putu.mardana@undiksha.ac.id[3]

**Abstrak**

Consumption of fossil fuels causes greenhouse effect and global warming, hence the need for renewable energy sources that are environmentally friendly. Hydrogen is one of the abundant elements on earth. Hydrogen refers to a clean and renewable energy source, hydrogen can be a good choice to reduce greenhouse gas emissions. One way to produce hydrogen is by electrochemical water splitting. This study aims to determine the characterization of iron-based nanomaterials (iron sulfide - iron hydroxide) as a water splitting catalyst in general. Iron sulfide synthesis was carried out using hydrothermal sulfidation method for 6 hours at 80 oC with nickel foam as substrate. Synthesis of iron sulfide varying the concentration of sodium sulfide nonahydrate (0.0125 M, 0.025 M, 0.05 M and 0.1 M) produced brownish yellow to blackish grey colored samples. Characterization results using XRD showed that iron sulfide peaks were detected at higher concentrations of sodium sulfide nonahydrate. Based on the results of analyzing iron hydroxide using SEM, it is known that the sample is in the form of nano walls and on iron sulfide, it is known that the sample is in the form of nanoscale particles. Based on electrochemical measurement results, iron hydroxide can be a good catalyst for hydrogen evolution reaction (HER) compared with commercial Pt/C. The overpotential of iron hydroxide is smaller than Pt/C, which is only 15 mV at a current density 10 mA/cm2 and iron sulfide can be a good catalyst for oxygen evolution reaction (OER) with electrocatalytic measurement results close to commercial RuO2. This is indicated by the small overpotential (260 mV at current densisty 10 mA/cm2 and small tafel slope (51 mV/dec).

**Kata Kunci:** Iron sulfide, iron hydroxide, electrocatalyst, water splitting, hydrothermal

## INTRODUCTION

Fossil fuels are still the main energy source to meet rapid industrialization and population growth. More than three-quarters of global energy production is generated by fossil fuels (i.e. oil, gas, and coal) and the remainder is provided by nuclear and other non-conventional or renewable energy sources [1]. The main problem with fossil fuels is that they are limited, non-renewable, and are the main source of $CO_2$ emissions into the atmosphere [1]. Non-renewable fossil fuels are increasingly depleting due to limited resources and concern for the environment, requiring exploration of alternative energy sources [2]. Apart from that, the use of fossil fuels is one of the causes of global warming. Therefore, it is necessary to analyze energy demand trends and strategies to separate energy production from greenhouse gas emissions presented from the perspective of innovative materials and technological solutions

needed to realize the transition to environmentally friendly energy [3]. Hydrogen is one of the most abundant elements in the world, it is found everywhere: in the air, the land, and water [4]. Hydrogen ($H_2$) refers to a clean and renewable energy source, Hydrogen as a good option for reducing greenhouse gas emissions [5, 6]. Hydrogen can be produced from various energy sources, including renewable energy [7]. Hydrogen does not produce harmful emissions, which is one of the biggest drawbacks of fossil fuels, and the calorific value of hydrogen is three times higher than that of petroleum [8]. Hydrogen can be used profitably in all sectors of the economy (as an industrial raw material, as a fuel for cars, and as an energy carrier in sustainable energy systems to generate electricity and heat through fuel cells [7].

One of the main problems facing hydrogen energy developers is the high cost of producing and storing hydrogen [9]. As a result, the current price of hydrogen fuel is still very high and less competitive than current conventional fuel [9]. Currently the focus of researchers is effective, efficient and environmentally friendly hydrogen production [9]. So it can produce hydrogen in large quantities and at low production costs [9]. There are several important components in hydrogen production by electrochemical means (water splitting), namely: electrolyte, cathode, anode and catalyst [7]. Electrochemical energy conversion systems provide a reliable solution to achieve the activation and transformation of energy-related small molecules under ambient conditions, for example, hydrogen evolution reaction (HER) and oxygen evolution reaction (OER) [10]. Electrochemical water splitting is a promising approach for $H_2$ production, which is sustainable and pollution-free [11]. Harvesting and converting energy from the environment through various green energy systems for water splitting can efficiently reduce external power consumption and various environmentally friendly energy systems to produce $H_2$ efficiently, one of which is water electrolysis with two electrodes [11].

Water splitting requires materials that can catalyze the hydrogen evolution reaction (HER) and oxygen evolution reaction (OER) efficiently [12]. Generally, an electrochemical water splitting cell involves two half reactions: the oxygen evolution reaction (OER) at the anode side and hydrogen evolution reaction (HER) at the cathode [13]. So far, commercial electrochemical water splitting for mass hydrogen production has been limited because of the large overpotentials required (>1.5 V, and the theoretical minimum value is 1.23 V) [13]. In addition, the process of splitting hydrogen and oxygen atoms requires more energy than can be obtained from burning hydrogen itself, so it requires an energy source that is abundant and does not damage the environment which can break down water molecules [4]. The ideal bifunctional electrocatalyst water splitting should be a low-cost, highly active and economical preparation method, which can provide long-term stability for the oxygen evolution reaction (OER) and hydrogen evolution reaction (HER) in the electrolyte [11].

Transition metal compounds are considered as alternative catalysts for alkaline water electrolysis, due to their excellent performance, cost efficiency, structural diversity and when synthesized they act as binder-free electrodes [14]. Sulfide-based compounds show promise in overall water splitting due to their high electronic conductivity [14]. In addition, transition metal sulfides can also replace noble metals in catalyzing overall water separation, and it was found that S anions can effectively optimize proton adsorption and stimulate OOH deprotonation simultaneously [15]. Iron-based sulfides have various phases, including FeS, $FeS_2$, and $Fe_3S_4$, which have great application prospects in the fields of electrochemistry and catalytics [16]. Based on this, it is considered to develop active Fe-based electrocatalytic materials, especially Fe-S-based catalysts for general water splitting and using nickel foam as a substrate. Nickel foam (NF) as a cheap commercial material can be used as an electrode substrate, its high electronic and ionic conductivity makes it an excellent electrode material [17]. In addition, the three-dimensional (3D) open porous structure of NFs provides a high surface area that maximizes contact between the electrolyte material and the electrode [18].

One method that can be used to develop Fe-S based catalysts is Hydrothermal. The hydrothermal method works on applying wet-chemical techniques for crystallizing the materials to a nanostructure [19]. Besides allowing controllable material characteristics with stoichiometry, hydrothermal synthesis offers additional substantial benefits such as operating at low synthesis temperature, fast and flexible continuous or batch processing, large scale industrial production, cleaner processing routes, and not involving harmful organic solvents [20]. Consequently, hydrothermal synthesis can be considered as a green and energy efficient process [20]. On the other hand, the liquid based methods can lead to improved control of the thermodynamics and kinetics involved in nucleation and growth processes [20]. Therefore, growing particles of varied morphologies in those methods can be achieved by altering thermodynamic and kinetic parameters such as temperature, concentration of reactants, duration of crystal growth, and additives [20].

In this research, sulfidation of iron based nanomaterials was carried out using a multipurpose hydrothermal method that is simple, easy to operate and fast to directly synthesize iron sulfide - iron hydroxide composite materials on nickel foam ($Fe_xS_y$ /$Fe(OH)_2$ @NF) by varying the concentration of Sodium Sulfide Nonahydrate. Then material analysis was carried out to determine the morphology of ($Fe_xS_y$ /$Fe(OH)_2$ @NF) and electrochemical tests to determine the electrocatalytic activity of ($Fe_xS_y$ /$Fe(OH)_2$ @NF) as a catalyst for water splitting.

## RESEARCH METHODS

### 2.1 Materials and Reagents.

$FeSO_4$ as much as 0.695 grams (concentration: 0.0625 M, FW: 278.02, DI water 40 mL), Ammonia ($NH_4OH$) as much as 20 mL, clean nickel foam (NF) as substrate, DI water, $Fe(OH)_2$ 30 seconds, Sodium Sulfide Nonahydrate (MW: 240.18), 1.0 M KOH.

### 2.2 Synthesis of $Fe(OH)_2$/NF.

Synthesis of $Fe(OH)_2$ using Chemical Bath Deposition (CBD) method. $FeSO_4$ with concentration: 0.0625 M, FW: 278.02 was mixed with 40 mL of DI water, resulting in 0.695 grams of $FeSO_4$. After that, put it into ultrasonic to mix the chemicals together. Then prepare water with a temperature of 10 $^oC$. After the $FeSO_4$ has been mixed, put it in 10 $^oC$ water. Then put NF into the plasma cleaner for 3 minutes and put the NF into the $FeSO_4$ (this process is carried out at a temperature of 10 $^oC$). After that mix 2 mL $NH_4OH$ with $FeSO_4$/NF with for 30 seconds. After that, dry it in the oven for approximately one day and we have obtained $Fe(OH)_2$.

$$2NH_4OH + FeSO_4 \longrightarrow Fe(OH)_2 + (NH_4)_2SO_4$$

### 2.3 Synthesis of $Fe_xS_y$/NF

The synthesis of $Fe_xS_y$ used the hydrothermal sulfidation method with four different concentrations of Sodium Sulfide Nonahydrate. First, prepare Sodium Sulfide Nonahydrate with concentrations of 0.0125 M, 0.025 M, 0.05 M and 0.1 M which are then mixed with 40 mL of DI water respectively. Second, prepare the $Fe(OH)_2$/NF surface using a plasma cleaner. Third, add $Fe(OH)_2$/NF to the Teflon which already contains Sodium Sulfide Nonahydrate and DI water. Fourth, put the tflon into the autocalve and close it tightly, then put it in the furnace at a temperature of 80 $^oC$ so that it undergoes a hydrothermal process. With 1 hour heating, 6 hours annealing and natural cooling. After the hydrothermal sulfidation process is complete, the sample is removed and dried again using an oven.

$$Fe(OH)_2 + Na_2S{\cdot}9H_2O \longrightarrow Fe_xS_y + 2NaOH$$

### 2.4 Materials Characterization

Composition and crystal phase of various samples were determined using X-ray diffractionmeter (XRD) (λ=0.15406 nm). The microscopic morphology of electrocatalyst was examined on field-emission scanning electron microscopy (FESEM, Hitachi S-4800). And using Raman spectroscopy to find out detailed information about chemical structure, phase and polymorphy, crystallinity and molecular interactions.

### 2.5 Electrochemical measurements

Electrochemical measurements to determine the electrocatalytic activity of ($FeS/Fe(OH)_2$ @NF) as a catalyst for water splitting. There are three types of tests that will be carried out for electrochemical measurements, such as: LSV OER and HER, EIS OER and HER, ESCA OER and HER for each sample. In the electrochemical test, the working electrode used is $FeS/Fe(OH)_2$ @NF, the reference electrode is SCE and the counter electrode is Pt.

## RESULTS AND DISCUSSION

### 3.1 Synthesis Result of Iron Sulfide – Iron Hydroxide.

The synthesis of $Fe_xS_y$ with four different concentrations of Sodium Sulfide Nonahydrate has been successfully carried out using the hydrothermal sulfidation method. Before carrying out the $Fe_xS_y$ synthesis, iron hydroxide was first synthesized using the chemical bath deposition (CBD) method with nickel foam (NF) as the substrate. $FeSO_4$/NF was mixed with 2 mL of $NH_4OH$ for 30 seconds. Then dried in the oven for approximately one day and obtained iron hydroxide with a brownish yellow color as seen in Figure 1.

**Figure 1. Synthesis result of iron hydroxide.**

The synthesis of $Fe_xS_y$ was carried out by mixing $Fe(OH)_2$ into four teflons which already contained Sodium Sulfide Nonahydrate, each teflon having a different concentration (0.0125 M, 0.025 M, 0.05 M and 0.1 M). Next, the teflon is put into an autoclave and a hydrothermal sulfidation process is carried out using a furnace at a temperature of 80 $^oC$ with a heating process of 1 hour, annealing for 6 hours, and natural cooling. After the hydrothermal sulfidation process was complete, the sample was removed and dried again using an oven for approximately one day. The $Fe_xS_y$ synthesis results obtained have different colors, as seen in Figure 2.


Figure 2. Synthesis result of iron sulfide

Sampel 1 is $Fe_xS_y/NF$ ($Na_2S \cdot 9H_2O : 0.0125$ M), sampe 2 is $Fe_xS_y$ ($Na_2S \cdot 9H_2O : 0.025$ M), sampel 3 is $Fe_xS_y$ ($Na_2S \cdot 9H_2O : 0.05$ M) and sampe 4 is $Fe_xS_y$ ($Na_2S \cdot 9H_2O : 0.1$ M). In sample 1 with a concentration of 0.0125 M Sodium Sulfide Nonahydrate has the brightest color and is most similar to $Fe(OH)_2$. Meanwhile, sample 4 with a concentration

of 0.1 M Sodium Sulfide Nonahydrate has the darkest color. The higher concentration of Sodium Sulfide Nonahydrate produces a darker sample color.

### 3.2 Characterization Result Using XRD

The crystal structure of iron hydroxide and iron sulfide nanomaterials was investigated using X-Ray Diffraction (XRD) and the results are shown in Figure 24. The samples were tested at 2θ angles ranging from 5º to 90º with Cu as the x-ray source (λ = 1.5406 Å). The resulting XRD data was then phase identified qualitatively using Origin software. In addition to finding out information about the composition of materials and the structure of atoms or molecules in materials, XRD is also used to find out whether a crystal is pure and represents an easy system for analyzing synthesized materials. In distinguishing and analyzing unknown crystals using JCPDS cards.

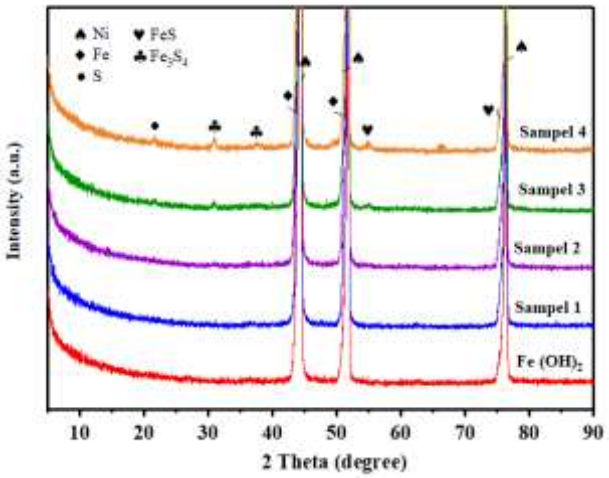


**Figure 3. XRD patterns of iron sulfide**

Sampel 1 is $Fe_xS_y/NF$ ($Na_2S \cdot 9H_2O : 0.0125$ M), sampel 2 is $Fe_xS_y$ ($Na_2S \cdot 9H_2O : 0.025$ M), sampel 3 is $Fe_xS_y$ ($Na_2S \cdot 9H_2O : 0.05$ M) and sampel 4 is $Fe_xS_y$ ($Na_2S \cdot 9H_2O : 0.1$ M). The XRD results show that the diffraction peaks (for all samples) that stand out at an angle of 2θ are 44.34606º, 51.55459º and 76.0163º which have high intensity. At the angles 44.34606º and 51.55459º it contains the elements Ni (JCPDS card No. 04-0850) and Fe (JCPDS card No.52-05135), while at the angle 76.0163º it contains the elements Fe (JCPDS card No.52-05135) and FeS (JCPDS card No. 15-0037) [21, 22]. Other peaks have low intensity at angle 2θ (21.82763º, 31.07134º, 37.5577 and 54.96846º). Sample 3 and sample 4 not only show the diffraction peaks of FeS (JCPDS card No. 15-0037) and $Fe_3S_4$ (JCPDS card No. 16-0713), but also the S peak (JCPDS card No. .34-0941) [21, 23].

### 3.3 Characterization Result Using FE SEM

The morphology of the iron hydroxide nanomaterial synthesized using the chemical bath deposition (CBD) method was investigated using Scanning Electron Microscopy (SEM) and the results are shown in Figure 25. SEM imaging results show the morphology of the iron hydroxide nanomaterial in the form of nanowalls. Meanwhile, the morphology of iron sulfide nanomaterials synthesized at 80 ºC for 6 hours using the hydrothermal sulfidation method with four different concentrations of Sodium Sulfide Nonahydrate (0.0125 M, 0.025 M, 0.05 M and 0.1 M) was investigated by Scanning Electron Microscopy. (SEM) and the results are shown in Figures 25 to 26. The image represents the morphological structure of iron sulfide with magnifications of 10000 times, 25000 times and 50000 times. The concentration of Sodium Sulfide Nonahydrate affects the morphology of iron sulfide and at low magnification we can see the uniformity of the sample.

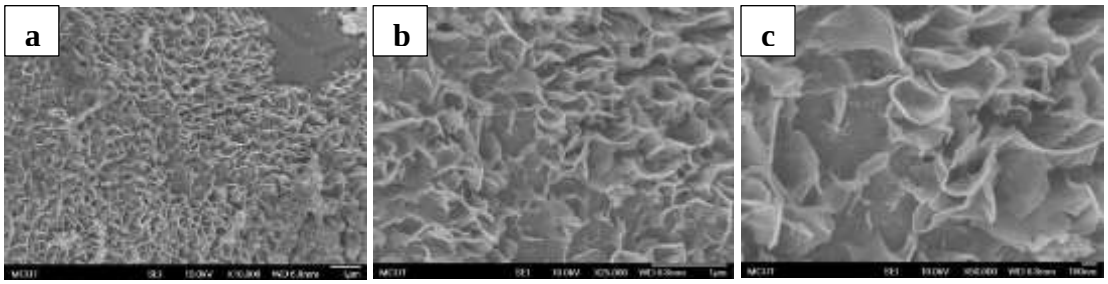


Figure 4. The morphological structure of iron hydroxide using SEM with different magnifications, (a) 10000x. (b) 25000x. (c) 50000x.

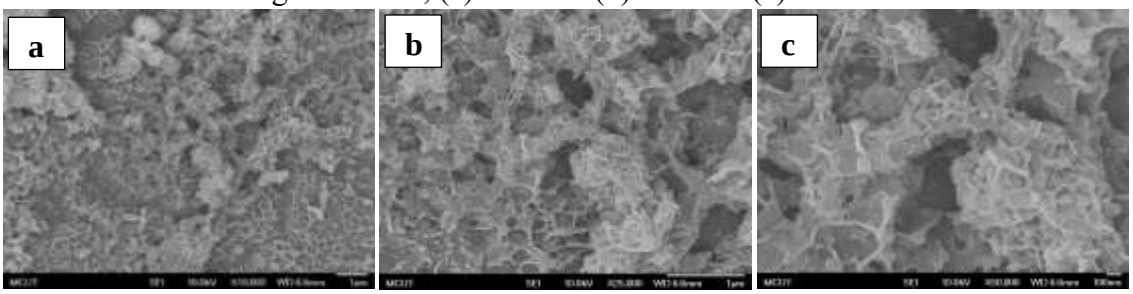


Figure 5. The morphological structure of iron sulfide (0.0125M sodium sulfide nonahydrate) using SEM with different magnifications, (a) 10000x. (b) 25000x. (c) 50000x.

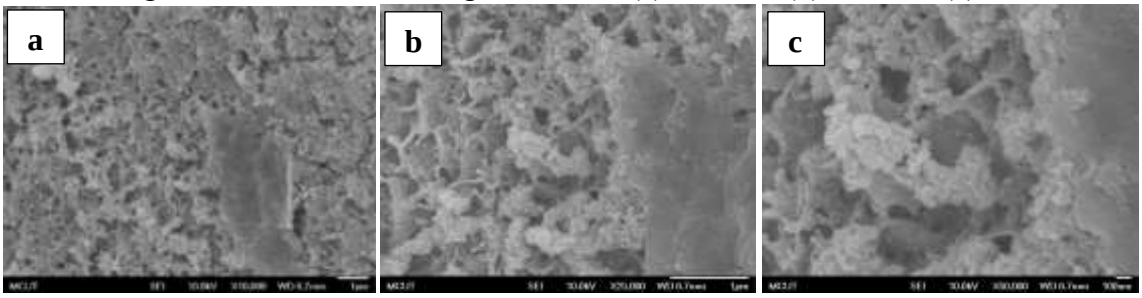


Figure 6. The morphological structure of iron sulfide (0.025M sodium sulfide nonahydrate) using SEM with different magnifications, (a) 10000x. (b) 25000x. (c) 50000x.

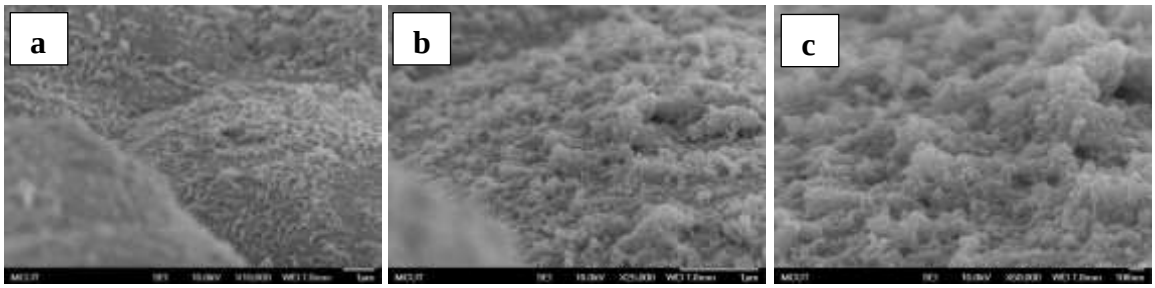


Figure 7. The morphological structure of iron sulfide (0.05M sodium sulfide nonahydrate) using SEM with different magnifications, (a) 10000x. (b) 25000x. (c) 50000x.

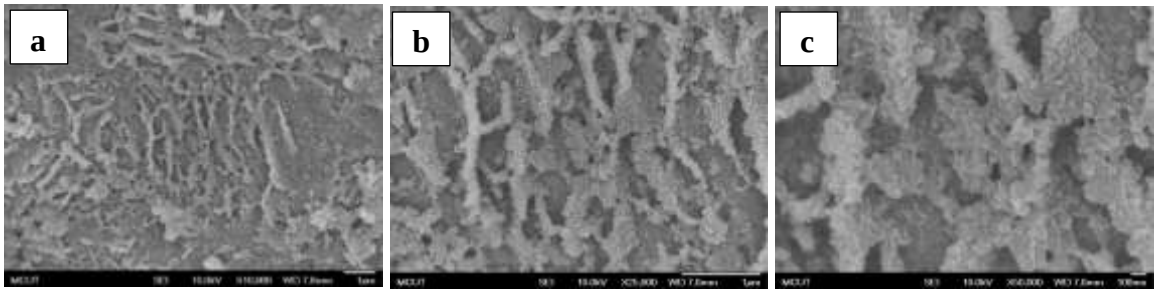

Figure 8. The morphological structure of iron sulfide (0.1M sodium sulfide nonahydrate) using SEM with different magnifications, (a) 10000x. (b) 25000x. (c) 50000x.

### 3.4 Electrocatalytic Activity Result Using Electrochemical Measurement

Electrochemical measurements were carried out in a standard three-electrode cell. A Pt plate was used as the counter electrode and a saturated calomel electrode (in saturated KCl) as the reference electrode. All potentials are calculated with respect to the reversible hydrogen electrode (RHE) and the overpotential (η) is calculated by η (V) = E (RHE) - 1.23V. Figures 9 to 12 compare the catalytic performance of iron hydroxide and iron sulfide with four different concentrations of Sodium Sulfide Nonahydrate (0.0125 M, 0.025 M, 0.05 M, and 0.1 M) for overall water splitting in 1 M KOH.

#### 3.4.1 Linear Sweep Voltametry (LSV)

Linear sweep voltammetry (LSV) measurements were recorded at a scan rate of 1 mV/s. The overpotential value of iron sulfide nanomaterials ware analyzed using LSV curves. The LSV curve shown in Figure 9 and Figure 10 is a curve that has been corrected with IR compensation. The overpotential and tafel slope values indicate the electrocatalytic performance of material. Small overpotential and tafel slope values indicate good electrocatalyst performance [24, 25]. In figure 30 for the oxygen evolution reaction (OER), it can be seen that $Fe_xS_y$ $(Na_2S \cdot 9H_2O : 0.1\ M)$ has smallest overpotential and tafel slope among the other samples. The tafel slope value for $Fe_xS_y$ $(Na_2S \cdot 9H_2O : 0.1\ M)$ is 51 mV/dec. At a current density of 10 mA/cm$^2$ the overpotential value of $Fe_xS_y$ $(Na_2S \cdot 9H_2O : 0.1\ M)$ is 260 mV and at a current density of 100 mA/cm$^2$ the overpotential value is 382 mV. At a current density of 10 mA/cm$^2$, $Fe_xS_y$ $(Na_2S \cdot 9H_2O : 0.1\ M)$, (η = 260 mV) shows lower overpotential compared to the widely used commercial $RuO_2$ catalyst. In figure 31 for the hydrogen evolution reaction (HER), it can be seen that iron hydroxide ($Fe(OH)_2$) has smallest overpotential than the other samples. At a current density of 10 mA/cm$^2$ the overpotential value of iron hydroxide ($Fe(OH)_2$) is 15 mV and at a current density of 100 mA/cm$^2$ the overpotential value is 97 mV. At a current density of 10 mA/cm$^2$, iron hydroxide ($Fe(OH)_2$), (η = 15 mV) show lower overpotential compared to the widely used commercial Pt/C catalyst.

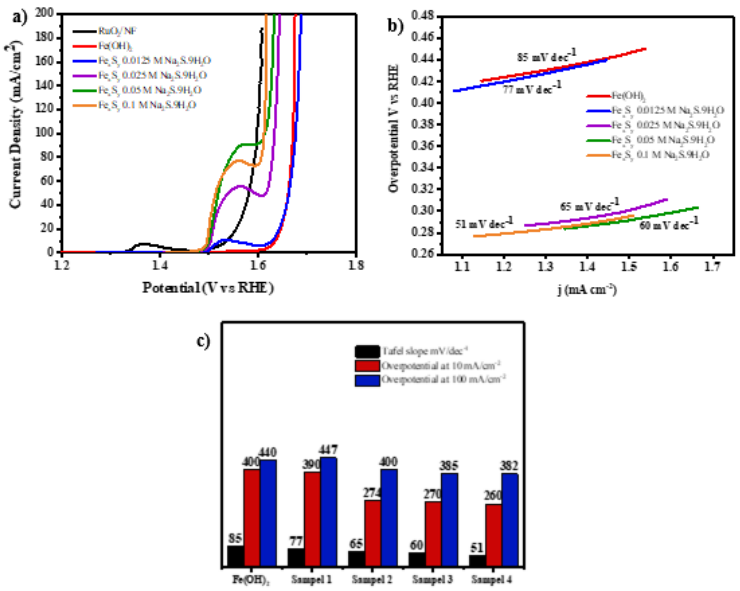


Figure 9. (a) LSV for OER with IR compensation. (b) Tafel slope for OER. (c) OER performance comparison between tafel slope (mV/dec) and overpotential (mV).

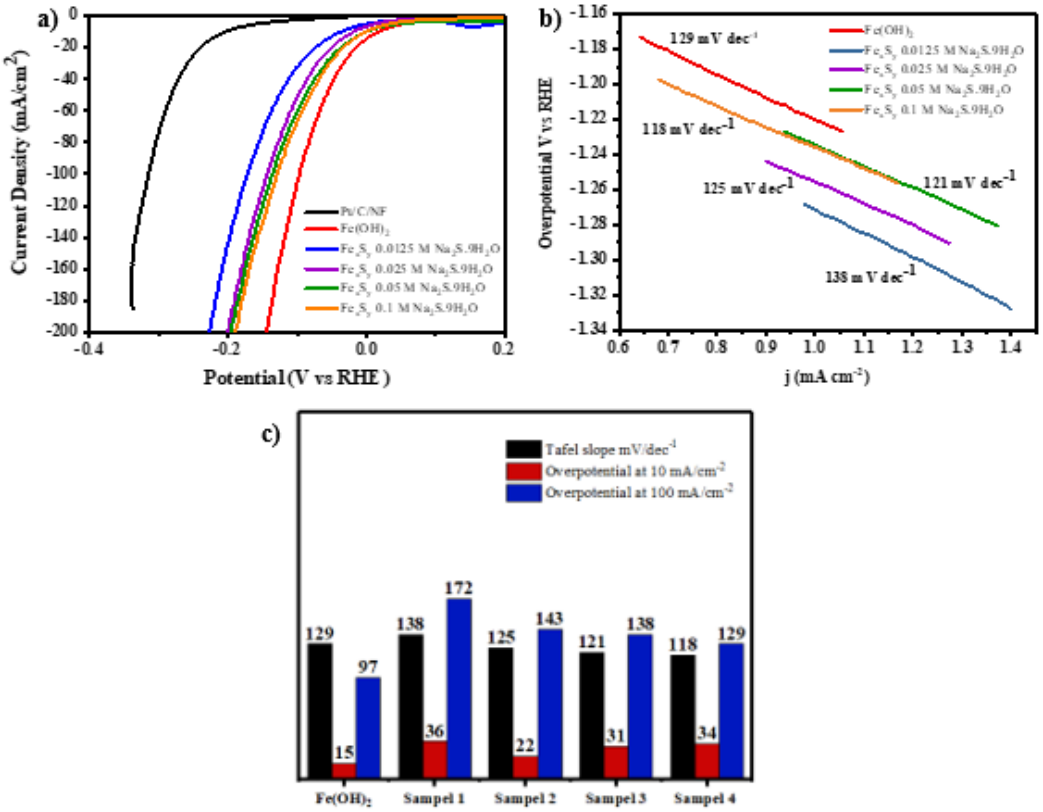


Figure 10. (a) LSV for HER with IR compensation. (b) Tafel slope for HER. (c) HER performance comparison between tafel slope (mV/dec) and overpotential (mV).

### 3.4.2 Electrochemical Impedance Spectroscopy (EIS)

The reaction kinetics of the electrode interface were also studied by Electrochemical Impedance Spectroscopy (EIS) was performed at overpotential of 100 mV. Based on the diameter of the semicircle in the Nyquist diagram for OER (which was analyzed using OriginPro software), the charge transfer resistance ($R_{ct}$) $Fe_xS_y/NF$ ($Na_2S \cdot 9H_2O : 0.0125$ M) ($R_{ct} = 3.26\ \Omega$) < $Fe_xS_y$ ($Na_2S \cdot 9H_2O : 0.1$ M) ($R_{ct} = 3.41\ \Omega$) < $Fe_xS_y$ ($Na_2S \cdot 9H_2O : 0.05$ M) ($R_{ct} = 4.14\ \Omega$) < $Fe_xS_y$ ($Na_2S \cdot 9H_2O : 0.025$ M) ($R_{ct} = 4.58\ \Omega$) < $Fe(OH)_2$ ($R_{ct} = 32.36\ \Omega$) was obtained (Figure 11.a). In addition, based on the diameter of the semicircle in the Nyquist diagram for HER (which was analyzed using OriginPro software), the charge transfer resistance ($R_{ct}$) $Fe_xS_y/NF$ ($Na_2S \cdot 9H_2O : 0.0125$ M) ($R_{ct} = 0.59\ \Omega$) < $Fe_xS_y$ ($Na_2S \cdot 9H_2O : 0.025$ M) ($R_{ct} = 0.69\ \Omega$) < $Fe_xS_y$ ($Na_2S \cdot 9H_2O : 0.05$ M) ($R_{ct} = 1.20\ \Omega$) < $Fe_xS_y$ ($Na_2S \cdot 9H_2O : 0.1$ M) ($R_{ct} = 1.38\ \Omega$) < $Fe(OH)_2$ ($R_{ct} = 7.70\ \Omega$) was obtained (Figure 11.b).

### 3.4.3 Electrochemical Active Surface Area (ECSA)

The electrochemical active surface area of the electrocatalyst (ECSA, represented by the electrochemical double layer capacitance $C_{dl}$) to further evaluate the intrinsic activity of the catalyst. ECSA was measured at five scan rates (10, 30, 50, 70 and 90) mV/s and analyzed using OriginPro software. As shown in figure 33 the double layer capacitance ($C_{dl}$) of Fe(OH)2 is higher compared to the other samples, namely 67.21 mF/cm$^2$ for OER and 58.28 mF/cm$^2$ for HER (Figure 12). Where the electrochemical double layer capacitance ($C_{dl}$) is directly proportional to the electrochemically active surface area (ECSA).

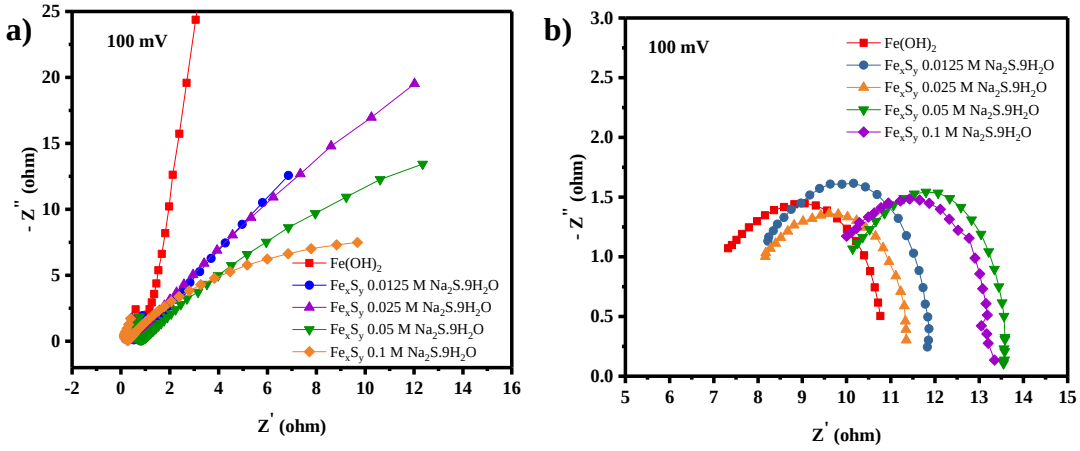


Figure 11. Electrochemical impedance spectra measured at overpotential of 100 mV, (a) for OER. (b) for HER

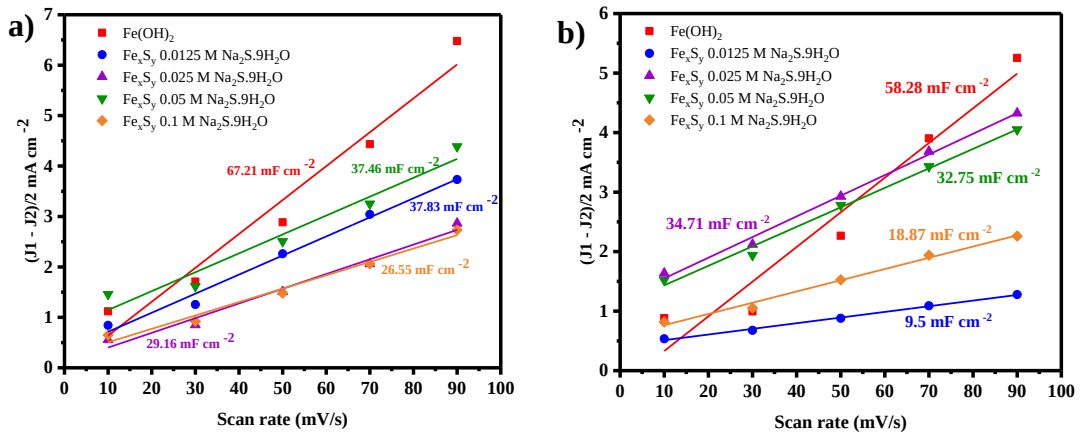


Figure 12. Electrochemical Active Surface Area in five scan rate (10,30,50,70 and 90) mV/s, (a) for OER. (b) for HER

### 4.1 Synthesis Result of Nanomaterial Iron Sulfide

Based on the results of the analysis of all samples, it is known that the iron sulfide produced has a different color. Sample 1 (0.0125 M) and sample 2 (0.025 M) with a lower concentration of Sodium Sulfide Nonahydrate have a lighter color. Meanwhile, sample 3 (0.05 M) and sample 4 (0.1 M) with a higher concentration of Sodium Sulfide Nonahydrate have a darker color. Iron sulfide has varying colors (from yellowish gold, brown to blackish gray) depending on temperature, crystallinization process, ions and environmental conditions. The colors produced from these samples are brownish yellow (sample 1), gray (sample 2) and blackish gray (sample 3 and sample 4).

In the synthesis of iron hydroxide $FeSO_4$ is the main Fe ion contributor which interacts with the nickel foam and etches the nickel foam to change the surface of the nickel foam. Iron ions can form bonds with the surface of the nickel foam or help in the formation of compounds between $NH_4OH$ and the surface of the nickel foam to form iron hydroxide. In the synthesis of iron sulfide, the surface of the iron hydroxide is modified by chemical deposition using the

hydrothermal method. The reaction between iron hydroxide and nonahydrate sodium sulfide produces iron sulfide precipitates, which form a layer on the surface of the iron sulfide. The amount of sulfide ions available in solution is affected by the concentration of $Na_2S \cdot 9H_2O$, which can also affect the physical and chemical properties of iron sulfide precipitates [26]. The amount of sulfide ions available to react with iron hydroxide is greater at high $Na_2S \cdot 9H_2O$ concentrations. This results in a thicker and denser iron sulfide precipitate, so the color of the precipitate tends to be darker, with a color close to black or dark gray. At lower concentrations of $Na_2S \cdot 9H_2O$ results in the formation of iron sulfide deposits that are thinner or less dense. This is because the number of sulfide ions that react with iron hydroxide is less, resulting in a lighter color. The concentration of nonahydrate sodium sulfide affects the level of sulfide formed on the surface of the iron hydroxide, resulting in different colors.

**4.2 Characterization Result Iron Sulfide Using XRD**

XRD patterns are used to study the phase composition and crystallinity of the prepared materials. The results show that there are three strong diffraction peaks from the materials, namely at angles 44.34606$^o$, 51.55459$^o$ and 76.0163$^o$. The main peak not only contains Ni but also contains Fe because the Ni and Fe peaks are close together, resulting in a peak with a higher intensity. Of the four different concentrations of Sodium Sulfide Nonahydrate (0.0125 M, 0.025 M, 0.05 M and 0.1 M) given to iron hydroxide, sample 3 and sample 4 have the greatest sulfur content. It can be seen from the peaks formed, where sample 3 has a concentration of Sodium Sulfide Nonahydrate of 0.05 M and sample 4 has a concentration of Sodium Sulfide Nonahydrate of 0.1 M. Meanwhile in sample 1 (Sodium Sulfide Nonahydrate 0.0125 M) and sample 2 (Sodium Sulfide Nonahydrate 0.025 M) the resulting peak has a very low intensity making it difficult to identify. From these results it can be seen that the addition of Sodium Sulfide Nonahydrate concentrate can increase the sulfur content in the sample. By using a low temperature hydrothermal process the iron sulfides detected were troilite (FeS) and greigite ($Fe_3S_4$). There are no other impurity peaks in the material and it has good purity. This indicates that iron hydroxide has been successfully converted into iron sulfide during the hydrothermal process.

The peak intensity in the XRD pattern can often be increased by increasing the concentration of $Na_2S \cdot 9H_2O$. This is because when concentration rises, more iron sulfide precipitate is produced, leading to an increase in the number of crystals that contribute to X-ray diffraction. Greater peak intensities may be a sign that more crystals of iron sulfide are forming. The size and uniformity of the iron sulfide crystals that are generated can change when the concentration of $Na_2S \cdot 9H_2O$ is increased. Sharper XRD peaks and greater intensities are often produced by larger or more homogenous crystals. The iron sulfide XRD pattern may have weaker or less distinct peaks at too low concentrations or if the reaction is not complete. This could mean that there are fewer or less fully formed iron sulfide crystals.

**4.3 Characterization Result Iron Sulfide Using FE SEM**

Analysis using SEM aims to determine the surface morphology of iron hydroxide and iron sulfide nanomaterials. Based on the results of analyzing iron hydroxide using SEM with magnifications of 10000 times, 25000 times and 50000 times, it is known that the samples are in the form of nano walls. This structure, which has thin layers that resemble walls or nano walls structures, is formed through a chemical deposition process that involves the deposition of a solution containing iron ions and hydroxide groups on a substrate (nickel foam). The use of nickel foam as a substrate can help the formation of nano walls structures [27]. This is because nickel has good mechanical strength, which allows it to be a solid and stable substrate for the growth of nano walls structures. This is important because nano walls structures are often very small in size and can be susceptible to deformation or damage if the substrate is not strong enough. In addition, nickel can interact with various chemical compounds and can form strong bonds with many materials, including iron hydroxide. This allows good adhesion

between the nickel substrate and the iron hydroxide layer formed, which is conductive to good structural growth of the nano walls [28]. By having a nano walls structure, iron hydroxide has more active areas that can act as an electrocatalyst.

In iron sulfide analyzed using SEM with magnifications of 10000 times, 25000 times and 50000 times, it is known that the samples are in the form of small or nano particles with various shapes, including round, oval, or irregular. The nanoscale structure of these particles is formed through the hydrothermal process. Using hydrothermal process the reaction rate is usually slower, it allows the formation of smaller iron sulfide crystals that tend to have a more uniform morphology and larger surface area [29].

Increasing the concentration of $Na_2S \cdot 9H_2O$ affects the crystal morphology, structure homogeneity and porosity pattern [26]. At high concentrations, more sulfide ions are available to react with iron hydroxide, resulting in more iron sulfide precipitates. Larger precipitates tend to produce larger crystal structures. It can also affect the porosity of the iron sulfide precipitate. At higher concentrations, deposits tend to have smaller or fewer pores. Whereas at low concentrations fewer sulfide ions react with iron hydroxide which produces fewer iron sulfide precipitates so that the crystal structure tends to have larger or more pores. At optimal concentrations, the iron sulfide structure may be more homogeneous and uniform. This is because the right concentration can ensure that the reaction between sulfide ions and iron hydroxide occurs evenly throughout the solution, resulting in a uniform precipitate.

**4.4 Electrocatalytic Activity Result Using Electrochemical Measurement**

Firstly, the OER catalytic activity of the samples was analyzed using electrochemical measurements consisting of LSV, EIS and ECSA. Based on the analysis of electrochemical measurements for LSV, it was found that sample 4 iron sulfide with a concentration of nonahydrate sodium sulfide (0.1 M) had the smallest overpotential compared to other samples and commercial $RuO_2$ which was 260 mV at a current density of 10 mA/cm$^2$ and 382 mV at a current density of 100 mA/cm$^2$. Iron sulfide with 0.1 M concentration of sodium sulfide nonahydrate shows good catalytic performance compared to other samples. This is indicated by the small overpotential and small tafel slope (51 mV/dec). Furthermore, electrochemical impedance spectroscopy (EIS) was used to explore the important causes of OER activity and the obtained charge transfer resistance of iron sulfide with 0.05 M and 0.1 M concentration of sodium sulfide nonahydrate were Rct = 3.41 Ω and Rct = 3.26 Ω, respectively. Which both samples have the smallest resistance value among other samples. The low resistance value indicates that the electrochemical system has high conductivity [24]. This indicates that electrons can easily move through the electrochemical system, and a low resistance value can indicate that the electrochemical system is operating efficiently [24]. The active surface area was also examined to determine the electrocatalyst performance of the samples. Based on the results of the ECSA analysis expressed by the electrochemical double layer capacitance $C_{dl}$, it was found that iron hydroxide had the highest linear slope among the other samples at 67.21 mF/cm$^2$. High $C_{dl}$ value indicates that the electrode has a large surface area [15]. With a larger surface area, the electrode has more active sites in contact with the electrolyte, thus supporting electrochemical reactions. In addition, electrodes with high $C_{dl}$ values usually indicate good catalytic performance.

The catalytic activity of HER in the samples was also analyzed using electrochemical measurements consisting of LSV, EIS and ECSA. Based on the analysis of electrochemical measurements for LSV, it is found that iron hydroxide has the smallest overpotential compared to other samples and commercial Pt/C which is 15 mV at a current density of 10 mA/cm$^2$ and 97 mV at a current density of 100 mA/cm$^2$. However, the smallest tafel slope value belongs to iron sulfide with 0.1 M concentration of sodium sulfide nonahydrate which is 118 mV/dec while iron hydroxide has a tafel slope of 129 mV/dec. Furthermore, electrochemical impedance spectroscopy (EIS) was used to explore the important causes of HER activity and obtained the

highest charge transfer resistance of iron hydroxide Rct = 7.70 Ω than other samples. While the lowest value of charge transfer resistance is iron hydroxide with 0.0125 M concentration of sodium sulfide nonahydrate, which is Rct = 0.59 Ω. Although iron hydroxide can be said to be a good catalyst because it has a low overpotential value, the charge transfer resistance value of iron hydroxide is still greater than other samples. The high value of charge transfer resistance may also indicate that the electrochemical reaction on the electrode surface is slow [24]. The active surface area was also examined to determine the electrocatalyst performance of the samples. Based on the results of ECSA analysis expressed by the electrochemical double layer capacitance $C_{dl}$, it is found that iron hydroxide has the highest linear slope among other samples at 58.28 mF/cm$^2$. A high $C_{dl}$ value indicates that the electrode has a large surface area. With a larger surface area, the electrode has more active sites in contact with the electrolyte, thus supporting electrochemical reactions [15]. In addition, electrodes with high $C_{dl}$ values usually indicate good catalytic performance.

There are two things that differentiate this research from previous research. Firstly, this research produces iron hydroxide morphology in the form of nanowalls. This nanowall-shaped morphology will be very good for application as a catalyst for electrochemical water splitting. This is because nanowalls have more active sites that can react with the electrolyte. In addition, this research carried out variations in the concentration of nonahydrate sodium sulfide in the synthesis of iron sulfide. Which in previous research controlled temperature and pH to produce iron sulfide. Changes in the concentration of nonahydrate sodium sulfide affect the sulfide ion content in the sample. The iron sulfide produced in this research can be a good catalyst in green hydrogen production because of its advantages compared to other catalysts (especially precious metals). Apart from the relatively low cost and simple method, the resulting iron sulfide also has a good electronic structure which can provide the reactivity needed to facilitate the water splitting reaction. The electrons in iron atoms have a tendency to participate in redox reactions involved in the water fission process, while sulfur atoms can facilitate the absorption and release of water molecules. Although this research has produced a good iron sulfide catalyst, there are several things that require further research. (1) Iron sulfide has a tendency to corrode or degrade in harsh or variable reaction environments, which can reduce catalyst life and require more frequent replacement. (2) The reactivity of iron sulfide towards other components in the reaction environment, such as metal ions or oxygen compounds, can cause contamination or deactivation of the catalyst. This can cause its catalytic performance to decrease and require additional steps to maintain its stability. By conducting more in-depth research regarding this matter, we can produce water splitting catalysts for more efficient and effective green hydrogen production on a large scale.

## CONCLUSION

The synthesis of iron sulfide with four different concentrations of Sodium Sulfide Nonahydrate has been successfully carried out using the hydrothermal sulfidation method. The colors produced from these samples are brownish yellow (sample 1), gray (sample 2) and blackish gray (sample 3 and sample 4). The higher concentration of Sodium Sulfide Nonahydrate produces a darker sample color. The characteristics of iron sulfide nanomaterials from the synthesized samples can be shown from the results of XRD and FE SEM. The XRD results show that there are three strong diffraction peaks only containing Ni but also containing Fe because the Ni and Fe peaks are close together, resulting in a peak with a higher intensity. Based on the results of analyzing iron hydroxide using SEM, it is known that the samples are in the form of nano walls and in iron sulfide it is known that the samples are in the form of nanoscale particles. Increasing the concentration of $Na_2S \cdot 9H_2O$ affects the crystal morphology, structure homogeneity and porosity pattern. At high concentrations, more sulfide ions are available to react with iron hydroxide, resulting in more iron sulfide precipitates.

Larger precipitates tend to produce larger crystal structures and have smaller or fewer pores. At optimal concentrations, the iron sulfide structure may be more homogeneous and uniform. This is because the right concentration can ensure that the reaction between sulfide ions and iron hydroxide occurs evenly throughout the solution, resulting in a uniform precipitate. Based on the results of electrochemical measurements for the oxygen evolution reaction, iron sulfide with nonahydrate sodium sulfide concentration (0.1 M) shows good catalytic performance compared to other samples. This is indicated by the small overpotential and small tafel slope. Iron sulfide with 0.05 M and 0.1 M concentration of sodium sulfide nonahydrate has the lowest charge transfer resistance. The low resistance value indicates that the electrochemical system has high conductivity. In HER it is found that iron hydroxide has the smallest overpotential compared to other samples but the highest tafel slope value is owned by iron sulfide with 0.1 M concentration of sodium sulfide nonahydrate and the lowest charge transfer resistance is owned by iron sulfide with 0.0125 M concentration of sodium sulfide nonahydrate. Based on the results of ECSA analysis expressed by the electrochemical double layer capacitance $C_{dl}$, it is found that iron hydroxide has the highest linear slope among other samples. A high $C_{dl}$ value indicates that the electrode has a large surface area. In general, iron hydroxide can be a good catalyst for oxygen evolution reaction (HER) compared with commercial Pt/C and iron sulfide can be a good catalyst for hydrogen evolution reaction (OER) with electrocatalytic measurement results close to commercial $RuO_2$.

## BIBLIOGRAPHY


Delgado, D., G. Hefter, and M. Minakshi, Hydrogen Generation, in Advanced Structured Materials: Alternative Energies. 2013, Springer. p. 141-161.

Ng, K.H., et al., Photocatalytic water splitting for solving energy crisis: Myth, Fact or Busted. Chemical Engineering Journal, 2021. **417**.

Gielen, D., F. Boshell, and D. Saygin, Climate and energy challenges for materials science. Nature Materials, 2016. **15**.

Cruden, G., Energy Alternatives. 2005, United States of America: Thomson Gale.

Yao, Y., X. Gao, and X. Meng, Recent advances on electrocatalytic and photocatalytic seawater splitting for hydrogen evolution. International Journal of Hydrogen Energy, 2021. **46**(13): p. 9087-9100.

Hassan, Q., et al., Renewable energy-to-green hydrogen: A review of main resources routes, processes and evaluation. International Journal of Hydrogen Energy, 2023. **48**(46): p. 17383-17408.

Felseghi, R.-A., et al., Hydrogen Fuel Cell Technology for the Sustainable Future of Stationary Applications. Energies, 2019. **12**(23).

Manoharan, Y., et al., Hydrogen Fuel Cell Vehicles; Current Status and Future Prospect. Applied Sciences, 2019. **9**(11).

Le, T.T., et al., Fueling the future: A comprehensive review of hydrogen energy systems and their challenges. International Journal of Hydrogen Energy, 2023. **54**: p. 791-816.

Wang, Q., et al., Atomic-scale engineering of chemical vapor deposition grown 2D transition metal dichalcogenides for electrocatalysis. Energy and Environmental Science, 2020. **13**(6): p. 1593-1616.

Li, X., et al., Water Splitting: From Electrode to Green Energy System. Nano-Micro Letters, 2020. **12**(131).

Zou, X., et al., In Situ Generation of Bifunctional, Efficient Fe-Based Catalysts from Mackinawite Iron Sulfide for Water Splitting. Chem, 2018. **4**(5): p. 1139–1152.

Zhou, Y. and H.J. Fan, Progress and Challenge of Amorphous Catalysts for Electrochemical Water Splitting. ACS Materials Letters, 2020. **3**(1): p. 136-147.

Zhang, R., et al., Hydrolysis assisted in-situ growth of 3D hierarchical FeS/NiS/nickel foam electrode for overall water splitting. Electrochimica Acta, 2019.
Li, H., et al., Chrysanthemum-like FeS/Ni3S2 heterostructure nanoarray as a robust bifunctional electrocatalyst for overall water splitting. Journal of Colloid and Interface Science, 2021. **608**: p. 536-548.
Pan, K., et al., FeS2/C Nanowires as an Effective Catalyst for Oxygen Evolution Reaction by Electrolytic Water Splitting. Materials, 2019. **12**(3364).
Ding, Y., H. Li, and Y. Hou, Phosphorus-doped nickel sulfides/nickel foam as electrode materials for electrocatalytic water splitting. International Journal of Hydrogen Energy, 2018. **43**(41): p. 19002-19009.
Gadisa, B.T., et al., ZnO@Ni foam photoelectrode modified with heteroatom doped graphitic carbon for enhanced photoelectrochemical water splitting under solar light. International Journal of Hydrogen Energy, 2021. **46**(2): p. 2075-2085.
Dahiya, M.S., V.K. Tomer, and S. Duhan, Metal–ferrite nanocomposites for targeted drug delivery, in Applications of Nanocomposite Materials in Drug Delivery. 2018. p. 737-760.
Suvaci, E. and E. Özel, Hydrothermal Synthesis, in Encyclopedia of Materials: Technical Ceramics and Glasses. 2021. p. 59-68.
Jin, J., et al., A glassy carbon electrode modified with FeS nanosheets as a highly sensitive amperometric sensor for hydrogen peroxide. Microchimica Acta, 2017. **184**(5): p. 1389-1396.
Li, J., et al., Highly-Dispersed Ni-NiO Nanoparticles Anchored on an SiO2 Support for an Enhanced CO Methanation Performance. Catalysts, 2019. **9**(6).
Ding, C., et al., Magnetic Fe3S4 nanoparticles with peroxidase-like activity, and their use in a photometric enzymatic glucose assay. Microchimica Acta, 2015. **183**(2): p. 625-631.
Jiang, C., Novel electrocatalysts for the electrochemical and photoelectrochemical water oxidation reaction, in Department of Chemical Engineering. 2019, University College London: London.
Wu, H., et al., Electrocatalytic water splitting: Mechanism and electrocatalyst design. Nano Research, 2023. **16**(7): p. 9142-9157.
Noël, V., et al., FeS colloids – formation and mobilization pathways in natural waters. Environmental Science: Nano, 2020. **7**(7): p. 2102-2116.
Wang, D., et al., Nickel foam as conductive substrate enhanced low-crystallinity two-dimensional iron hydrogen phosphate for oxygen evolution reaction. Journal of Alloys and Compounds, 2021. **870**.
Wang, D., et al., When NiO@Ni Meets WS(2) Nanosheet Array: A Highly Efficient and Ultrastable Electrocatalyst for Overall Water Splitting. ACS Cent Sci, 2018. **4**(1): p. 112-119.
Yang, G. and S.J. Park, Conventional and Microwave Hydrothermal Synthesis and Application of Functional Materials: A Review. Materials (Basel), 2019. **12**(7).